

# Measurement of fast neutron removal cross sections for the elemental analysis of concrete

Naledi Segale<sup>1,\*</sup>, Tanya Hutton<sup>1</sup>, Sizwe Mhlongo<sup>1</sup>, Andy Buffler<sup>1</sup>

<sup>1</sup>Department of Physics, University of Cape Town, Cape Town, South Africa, 7700.

\*E-mail: [SGLNXX001@myuct.ac.za](mailto:SGLNXX001@myuct.ac.za)

**Abstract.** Concrete structures in nuclear power plants (NPPs) are exposed to extreme conditions causing degradation and composition changes over the reactor lifetime. To ensure compliance of existing concrete structures to nuclear regulations the radiation shielding properties, and subsequent elemental composition, need to be non-destructively determined. Previous work at the University of Cape Town has demonstrated the use of fast neutron transmission spectroscopy to determine the composition of a concrete sample with respect to the base ingredients, but there are many instances where a more generalized approach is required. In this work we utilise sand, one of the primary components of concrete, to demonstrate the extension of the technique to determining the proportion of silicon dioxide (SiO<sub>2</sub>) and calcium carbonate (CaCO<sub>3</sub>) in a well-characterised sample. Fast neutron transmission measurements were made with an EJ301 organic liquid scintillator for a collimated beam of <sup>241</sup>Am-<sup>9</sup>Be neutrons incident on samples of SiO<sub>2</sub>, CaCO<sub>3</sub> and sand. We present the initial analyses of the effective removal cross section, integrated over the full range of measured neutron energies. Future work will include the determination of the energy dependent cross sections of SiO<sub>2</sub> and CaCO<sub>3</sub>, and the elemental cross sections for C, O, Si and Ca, which will be used to de-convolve the composition of sand, and eventually concrete.

## 1. Introduction

Concrete is widely used in nuclear power plants (NPPs) because of its mouldability, simple manufacturing process, use of locally available materials, cheap production cost, good compression strength and excellent shielding property against gamma rays and neutrons [1]. The concrete structures in NPPs are often exposed to high stresses, prolonged high temperatures, and high levels of neutron and gamma ray radiation causing the concrete to degrade and change in composition over time. Of particular concern to neutron radiation shielding is the loss of water [2], and hence hydrogen, which is difficult to quantify non-destructively.

In South Africa, Eskom owns and operates the Koeberg NPP, which features two pressurized water reactors each delivering 970 MW gross power. The two units were commissioned in the 1980s and the current license is set to expire in 2024. There are plans in place to extend the design life of the Koeberg NPP by a further 20 years, overseen by the National Nuclear Regulator (NNR) [3]. Part of the process requires re-evaluation of the existing concrete structures, with respect to radiation shielding and structural properties.

### 1.1 Fast neutron transmission spectroscopy (FNTS)

Fast neutrons are useful for the analysis of bulk materials as they are highly penetrating, produce characteristic radiation signatures for each element and are particularly sensitive to low mass elements such as hydrogen. For beam of neutrons incident on a sample of interest, three major signatures are produced: transmitted neutrons; scattered neutrons; and gamma rays (prompt and delayed) [4, 5]. Measurement of these signatures, both in intensity and energy provides information on the nuclei with which neutrons have interacted. In fast neutron transmission spectroscopy (FNTS), the elemental composition of a sample can be determined from the analysis of transmitted neutron spectra through a sample. For a neutron beam incident on a sample, some proportion of neutrons interact with the material and are subsequently removed from the beam. The neutrons which are transmitted through the sample are then detected. The ratio of the incident fluence spectrum and transmitted fluence spectrum can be used to determine the composition of the sample through the use of the effective removal cross section [4].

### 1.2 Effective removal cross section

The effective removal cross section ( $\Sigma_R$ ) provides a measure of the neutron attenuation through a bulk sample and is highly specific for each element. The concept of  $\Sigma_R$  is often associated with the presence of hydrogen in sample of interest, however can be extended to non-hydrogenous samples, as long they provide sufficient moderation of the neutron beam. Furthermore, it is only valid for fast neutrons with neutron energies between 2 MeV and 12 MeV as  $\Sigma_R$  is approximately constant within this range [6]. The attenuation of a beam of fast neutrons through a bulk sample can be modelled by Eq. 1, where  $I(t)$  is the transmitted neutron intensity for a sample of thickness  $t$ , and  $I(0)$  is the incident neutron intensity. For a composite material, the effective removal cross section is related to a linear combination of the constituent parts as shown in Eq. 2, where  $m_k$  is the mass fraction of component  $k$ , with density  $\rho_k$  [7]:

$$I(t) = I(0) \exp(-\Sigma_R t) \quad (1)$$

$$\Sigma_R / \rho = \sum_k m_k (\Sigma_{R,k} / \rho_k) \quad (2)$$

The use of FNTS for concrete analysis has been previously demonstrated at the University of Cape Town, where the measured energy dependent effective removal cross sections for sand, cement and water were used to de-convolve the relative ratios in well characterized concrete samples [8]. However, the use of this technique is limited to new concrete installations, as it is necessary to also measure with the composite ingredients which often have a location dependence [9]. Proof-of-concept studies have been undertaken to investigate the use of elemental responses for both transmitted and scattered neutrons to generalize the technique, but experimental validation is still needed [7]. In this work we present the progress towards the experimental implementation of elemental analysis of complex materials such as concrete. In this first phase sand, one of the primary ingredients of concrete is utilised as the exemplar material since it is comprised of known ratios of  $\text{SiO}_2$  and  $\text{CaCO}_3$ .

## 2. Experimental method

The experimental implementation of fast neutron transmission spectroscopy requires a collimated beam of fast neutrons with a known distribution in energy and intensity, a sample with which the neutrons interact, and a neutron sensitive detector with appropriate analysis protocols to determine neutron energy spectra. For the present work, the resources available at the n-lab [10], a fast neutron laboratory at the University of Cape Town were utilised. The experimental set up is illustrated in Fig. 1.



**Figure 1.** Fast neutron transmission experimental set-up. A pencil beam of  $^{241}\text{Am-}^9\text{Be}$  neutrons is incident on the segmented container, where the shaded sections correspond to a measurement of 4.0 cm sample thickness. Transmitted neutrons are incident on a 2'' x 2'' EJ301 organic liquid scintillator detector.

### 2.1 $^{241}\text{Am-}^9\text{Be}$ neutron source

An  $^{241}\text{Am-}^9\text{Be}$  radioisotopic source was used, which produces  $\alpha$ -particles via the decay of  $^{241}\text{Am}$ , which may slow down and capture on  $^9\text{Be}$  to produce  $^{12}\text{C}$ , a neutron and a 4.43 MeV  $\gamma$ -ray. The energy spectrum of the produced neutrons ranges from thermal to approximately 11 MeV in the distribution shown in Fig. 2. The 220 GBq  $^{241}\text{Am-}^9\text{Be}$  source at the n-lab produces around  $10^7$  neutrons per second into  $4\pi$  steradians. A pencil beam (0.8 cm diameter) of  $^{241}\text{Am-}^9\text{Be}$  distributed neutrons, as indicated by the arrow in Fig. 1, is produced with a 1.0 m long HDPE collimator.

### 2.2 Samples

Samples of  $\text{SiO}_2$ ,  $\text{CaCO}_3$  and sand were prepared in a segmented container, with cross sectional area of  $5.0 \times 5.0 \text{ cm}^2$  and thicknesses of 2.0, 4.0 and 6.0 cm. The  $\text{SiO}_2$  used was in the form of glass beads with diameter  $< 1.0 \text{ mm}$  and  $\text{CaCO}_3$  as a fine powder. A representative sample of the sand was analyzed by X-ray fluorescence and was found to contain 78.5 %  $\text{SiO}_2$  and 18.6 %  $\text{CaCO}_3$  by mass, with the remaining 2.9 % consisting of all other major oxides with no single one exceeding 0.5 % [8]. The samples were placed within the neutron beam as shown in Fig. 1, and for each thickness the samples were freshly prepared, and the total mass recorded, to minimize changes in density due to settling.

### 2.3 EJ301 neutron detector

Neutrons transmitted through the sample were detected using a 2'' x 2'' EJ301 organic liquid scintillator optically coupled to an ETL 9214 12-stage photomultiplier tube and base supplied by Scionix, and operated at a negative bias of 1100 V. Both the anode and dynode signals were acquired using a CAEN DT5730 digitizer [12] and the QtDAQ [13] software. As the detector is sensitive to both neutrons and gamma rays, pulse shape discrimination (PSD) was implemented through QtDAQ to identify neutron only events using the fast anode signals [14]. Energy information on the recoiling particles was obtained from the pulse height of the dynode signals after amplification and shaping with an Ortec 113 preamplifier and 574 amplifier. A typical PSD plot for an  $^{241}\text{Am-}^9\text{Be}$  source measured with an EJ301 detector is shown in Fig. 3. The neutron only events are used to produce a neutron light output ( $L$ ) spectrum after calibration with a series of reference gamma ray sources, which are used as a measure of neutron intensity  $I(t)$  introduced in Eq. 1.

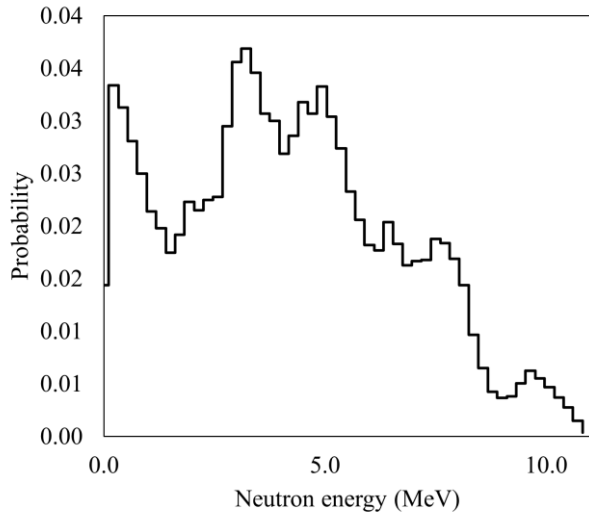


**Figure 2:** Neutron energy spectrum produced by an  $^{241}\text{Am}$ - $^9\text{Be}$  radioisotopic source [11].

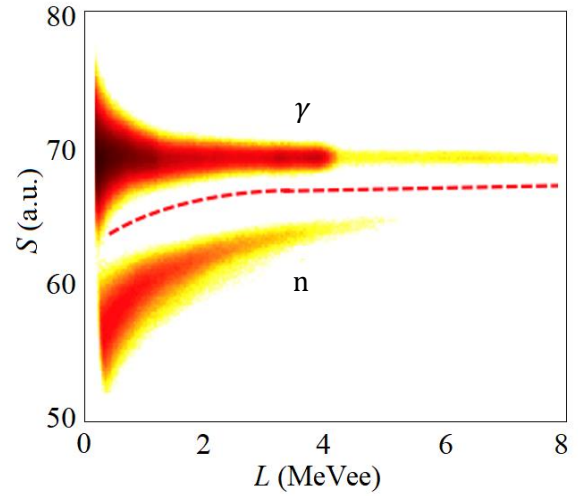


**Figure 3:** Counts as a function of light output parameter  $L$  and pulse shape parameter  $S$  measured with an EJ301 scintillator for an  $^{241}\text{Am}$ - $^9\text{Be}$  source. Contributions from neutrons ( $n$ ) and gamma rays ( $\gamma$ ), are separated by a software cut (dashed line)

### 3. Results and analysis

Calibrated neutron light output spectra measured for the three samples are shown in Fig. 4. In all instances the 0.0 cm case (no sample) is shown in black. As neutron attenuation is expected to behave according to Eq. 1, an increasing sample thickness should correspond to a reduction in measured neutron rate which is evident in the  $\text{SiO}_2$  and sand datasets. As the density of the  $\text{CaCO}_3$  sample is much lower than that of  $\text{SiO}_2$  or sand, the reduction in transmitted neutron rates is much lower.

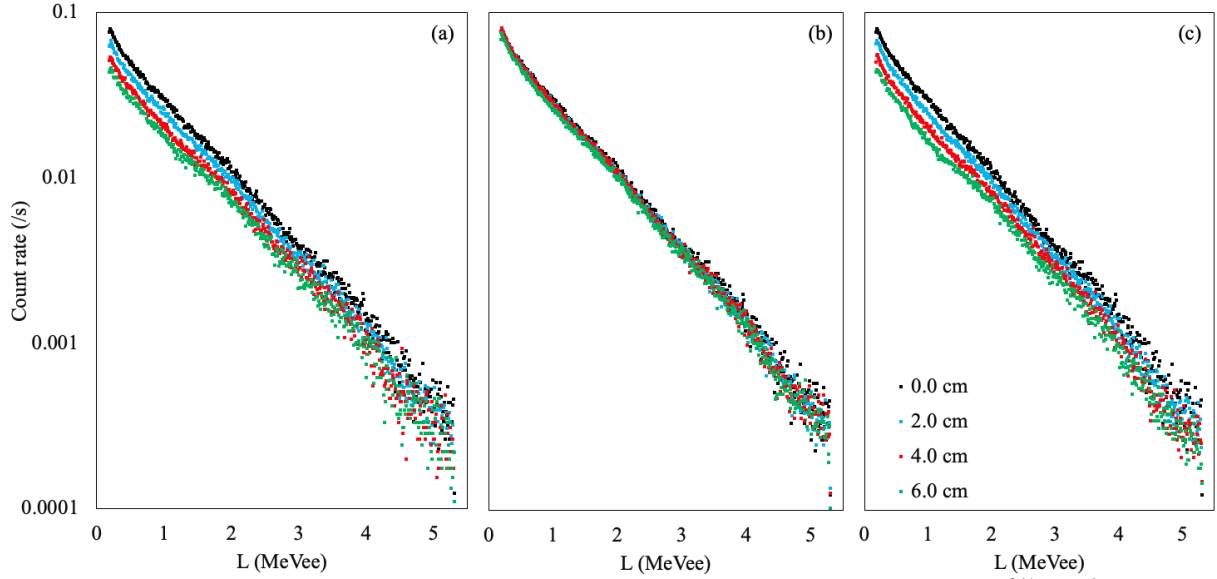


**Figure 4:** Light output spectra measured with EJ301 detector for neutrons from an  $^{241}\text{Am}$ - $^9\text{Be}$  source transmitted through samples (a)  $\text{SiO}_2$ , (b)  $\text{CaCO}_3$  and (c) sand measured and normalised with respect to measurement time.

To determine the effective removal cross section, the integrals of the measured light output spectra (Fig. 4) for the range of 1.0 – 5.5  $\text{MeV}_{\text{ee}}$  were used. The value for  $t = 0.0$  cm was taken to be the incident neutron intensity as no sample was present. Using these values  $\Sigma_R$  can be determined using Eq. 1, however as there are small variations in density  $\rho$  between sample preparations it is more useful to consider the parameter  $\Sigma_R/\rho$  for comparison. Table 1 contains a summary of the effective removal cross sections for  $\text{SiO}_2$ ,  $\text{CaCO}_3$  and sand averaged over the three non-zero thicknesses. The uncertainties presented correspond to the standard deviation of the mean as a full uncertainty analysis is still ongoing.

**Table 1:** Summary of removal cross section data for  $\text{SiO}_2$ ,  $\text{CaCO}_3$  and sand.

	$\Sigma_R$ [ $\text{cm}^{-1}$ ]		$\rho$ [ $\text{g cm}^{-3}$ ]		$\Sigma_R/\rho$ [ $\text{cm}^2 \text{g}^{-1}$ ]
	2.0 cm	4.0 cm : 6.0 cm	2.0 cm	4.0 cm : 6.0 cm	
<b><math>\text{SiO}_2</math></b>	0.085	0.084 : 0.081	1.40	1.45 : 1.42	$0.0586 \pm 0.0020$
<b><math>\text{CaCO}_3</math></b>	0.015	0.008 : 0.016	0.37	0.38 : 0.36	$0.034 \pm 0.013$
<b>Sand</b>	0.082	0.088 : 0.085	1.50	1.51 : 1.50	$0.0568 \pm 0.0015$

The data presented in Table 1 are taken over a broad range of energies and have limited usefulness in determining the ratios of  $\text{SiO}_2$  and  $\text{CaCO}_3$  in sand, however, if the ratios are already known then the process can be verified using Eq. 2. Using the measured  $\Sigma_R/\rho$  values, and the ratios of  $\text{SiO}_2$  and  $\text{CaCO}_3$  taken from previous XRF measurements,  $\Sigma_R/\rho$  for sand is determined to be  $0.0539 \pm 0.0030 \text{ cm}^2 \text{g}^{-1}$  which agrees with the measured value within uncertainties. It is noted that the removal cross section measured for 4.0 cm  $\text{CaCO}_3$  is lower than expected, and possible causes are still being investigated. As such, the calculated removal cross section for sand is marginally lower than the measured value, though there is still agreement between the measured and calculated values within the quoted uncertainties.

#### 4. Discussion and conclusion

The fast neutron transmission spectroscopy technique is being further developed to non-destructively determine the elemental composition of complex bulk materials such as concrete. In this work, the

removal cross sections were measured for sand, SiO<sub>2</sub> and CaCO<sub>3</sub> for <sup>241</sup>Am-<sup>9</sup>Be neutron energies. While the current uncertainty estimate for CaCO<sub>3</sub> is large, the results appear to be self-consistent.

The next phase of this research will require the use of spectrum unfolding to determine the energy dependence of the transmitted neutrons, and hence energy dependent removal cross sections. Additional measurements are underway with samples of C (graphite), and Si which are required to deconvolve the elemental composition of sand. After the technique is established for the elemental analysis of sand, more complex media such as concrete will be investigated.

## References

- [1] Basu P, Labbe P and Naus D, 2013. Nuclear Power Plant Concrete Structures. In: *Structural Mechanics in Reactor Technology*. IASMiRT, pp1-5
- [2] Peterson E, 1960. *Shielding Properties of Ordinary Concrete as a Function of Temperature*, USAEC, Report HW-65572
- [3] Department of Mineral Resources and Energy, 2019. Integrated Resource Plan (IRP2019)
- [4] Micklich B, Curry B, Fink C, Smith D and Yule T, 1994. System design considerations for fast-neutron interrogation systems. *Proceedings Substance of detection systems*, 2092, pp3-5
- [5] Buffler A, 1998. *Fast Neutron Scattering Analysis*. PhD thesis, University of Cape Town
- [6] El-Khayatt A, 2010. Calculation of fast neutron removal cross-sections for some compounds and materials. *Annals of Nuclear Energy*, **37**(2), pp218-222
- [7] Hutton T, Buffler A and Alexander M, 2022. Elemental analysis of concrete via fast neutron transmission and scattering spectrometry. *EPJ Web of Conferences*, **261**, 03003
- [8] Buffler A, Hutton T, Leadbeater T, Alexander M and Dlamini S, 2020. Neutron transmission studies for concrete used in the nuclear industry. *International Journal of Modern Physics: Conference Series*, **50**, pp3-8
- [9] Walker B, 2013. *Fine Aggregate Resources in the Greater Cape Town Area*. MSc thesis, University of Cape Town
- [10] Hutton T and Buffler A, 2017. A new D-T neutron facility at UCT. *SAIP2017 Proceedings*, pp324-330
- [11] International Standards Organisation, 1999. Neutron reference radiation fields, ISO 8529-1
- [12] CAEN SpA, 2021. User manual UM3148, DT5730/DT5730S – 8 Channel 14 bit 500/200 MS/s Digitizer
- [13] Comrie A, 2015. QtDAQ git repository, [online] Available: <https://bitbucket.org/veggiesaurus/qtdaq>
- [14] Comrie A, Buffler A, Smit F, and Wortche H, 2015. Digital neutron/gamma discrimination with an organic scintillator at energies between 1 MeV and 100 MeV *Nuclear Instrumentation and Methods*, **772**, pp43–49